

Numerical study of Fluid Flow and Heat Transfer Characteristics due to Air Jet Impingement in Food Cooling Process

Nur Mohammad*, Anzaman Hossen, Zahir U. Ahmed

Department of Mechanical Engineering, Khulna University of Engineering & Technology, Khulna-9203, BANGLADESH

ABSTRACT

When the temperature of the impinging fluid differs from that of the impingement surface, impingement cooling is extensively used to achieve high heat transfer rates. The surface heat transfer coefficient in impact cooling depends on several impact parameters, namely the design of the nozzle, the geometry of the object to be cooled, the exit distance of the beam from the object body, jet speed, and jet limit. Jet impingement is frequently used in a number of industrial settings to achieve high local heat transfer coefficients. This present work is about the air impingement cooling of hemispherical foodstuff, and it was done using ANSYS Fluent and computational fluid dynamics (CFD). As a Turbulence model, SST $k-\omega$ was employed. Several fluid flow regions were presented. Local Nusselt number distributions over the heated object's surface were studied for different Reynolds numbers (23,000–100,000), jet-to-cylinder distances (2–8), and surface curvature (0.57–1.14). The Nusselt number of stagnations increases as the Reynolds number increases, but reduces as the surface curvature increases and h/d has very little significance.

Keywords: Jet Impingement Heat Transfer, Cooling, Nusselt Number, Food, CFD

1. Introduction

Impingement cooling is a quick cooling technique that involves impinging high-speed, low-temperature air jets striking the item's surface symmetrically. Air impingement systems are a novel concept for reducing processing time. Jets of fluid impinge at high velocities on the surface of a product in impingement systems. Air impingement systems have been utilized in a variety of industrial applications, including textile and paper drying, electronic cooling, and glass quenching. Food cooling is critical in the food sector to avoid quality degradation. Crude or processed food should be put away at low temperatures. The growth of thermophilic and many mesophilic microorganisms may be induced by slow cooling. Many different sorts of cooling technologies are employed nowadays, and many of them take a lot of time and energy. Cooling with impinging jets results in a high rate of heat transfer, allowing the products to be quickly cooled to prevent this growth, as well as improved food quality and production pace. High-velocity air jets are directed perpendicular to the food surface during impingement freezing. The time it takes to freeze food is an important factor in food preservation. The fundamental benefit of this technique is that it increases the pace of heat transfer, allowing food to be frozen as soon as possible while maintaining its safety and quality. Given the thin boundary layer and the helpful impact of disturbance, impinging jets may accomplish wanted heat transfer rates with a flow a significant degree lower than a conventional parallel flow heat transfer system. It does not have to be a flat surface to be cooled; it can be round, cylindrical, hemispherical, elliptical, or any other irregular shape.

Jet impingement flows have been examined extensively in many research due to their wide range of applications, the majority of which is focused on flat targets surface and the convex or concave semi-circular target surface. In recent years, jet impingement cooling has become widely used in the food industry for freezing,

cooling, and thawing. This is due to the high heat transfer rates attained at the desired area. According to a study by Lujan et al., increasing drying air temperature essentially accelerated the drying rate for tortilla chips that were lacking in moisture due to air impingement [1]. Borquez et al. [2] studied the drying cycle of pressed fishcakes in different settings (mixing power, molecular size, dividers, temperature and found that temperature and molecular spacing affect the drying rate.

Scott and Richardson looked at how CFD can be used in food processing. Also, Xia and Sun discussed several food-related applications, as well as commercial codes and how to do a CFD study. Both studies discuss the benefits and downsides of CFD, as well as prospective CFD, uses in food systems [3, 4]. Marazani et al. [5] reviewed parameters that are affecting the performance of jet impingement on food cooling. Heat transfer rate on a surface under an impinging jet relies upon several parameters: Nusselt number (Nu), Reynolds number (Re), non-dimensional nozzle to surface spacing (H/D), and nozzle geometry.

The flow field around the object affects surface heat transfer. As a result, it is crucial to investigate the impingement system's flow field properties. To identify and archive the gliding of the round impact jet, Bouchez and Goldstein used the fog formed by the loss of dry ice pellets in the warm water in the pressure tank. [6] Cornaro et al. [7] used smoke red glide visualization to study the effect of spherical jets hitting convex and concave surfaces. The formation and increase of ring vortices in the jet shear layer and their interactions were shown in the jet. Gau and Chung used companion smoke particle technology to study glide patterns. The poor quality of the photographs made it difficult to assess the effects of curvature [8].

There is virtually little research on jet impingement cooling of hemispherical surfaces. San et al. [9] measured the local Nusselt number of a limited circular air jet

* Corresponding author. Tel.: +88-01888102868

E-mail addresses: nmnahid2@gmail.com

vertically impinging on a flat plate with a Reynolds number in the range of 30,000-67,000 and a H/d of 2. They discovered that the stronger the effect of surface heat flux on the Nusselt number, the higher the Reynolds number, and the greater the surface heating breadth, the lower the Nusselt number for a given jet hole diameter. The application of Jet Impingement for food cooling purposes has been studied by Carmela Dirita et al. The effect of localized forced convection via jet impingement has been documented, demonstrating how heat flow is considerably non-uniform over the cylinder surface and how the local Nusselt number is heavily reliant on the conjugate effect [10]. F.Gori and L.Bossi [11] examined the heat transfer of air slot jets impinging on the surface of a circular cylinder by forced convection for Reynolds numbers ranging from 4000 to 20000, with the cylinder having a diameter of D=10 mm and the slot jet having a height of S=5 mm. They found that decreasing the angle from the front impinging point reduces the local Nusselt numbers and proposed three empirical expressions. Olsson et al. [12], Singh and Singh [13], and others have statistically investigated the slot air jet impingement cooling of a circular cylinder. However, Nitin et al. and Kang et al. quantitatively examined jet impingement heating of a circular cylinder by a hot air jet. [14,15]. Qiang Guo et al. investigated the transient heat transfer of a circular air jet impinging on a finite-thickness flat plate with Reynolds numbers ranging from 14000 to 53000 [16]. Using transient heating liquid crystal technology, Reynolds numbers in the range of 5600 to 13200 and distances from the slit nozzle to the impact surface (Y / W) of 2 to 10 were studied by Chan et al. They found that the average number of nozzles around a semi-circular convex surface increased with increasing Reynolds number and decreased with increasing Y / W or S / W [17]. Lee et al. [18] measured local Nusselt number for an air jet impinging on a convex hemispherical surface; Re=11000-87000, L/d=2-10, and D/d=10.6 were used in the studies. It has been observed that the convex surface has a larger Nusselt number than the flat surface. A succession of three-dimensional counter-rotating vortices initiated on the convex wall may be to blame. These vortices can improve heat transmission by increasing momentum transport in the flow. However, this current study quantified the flow and heat transfer properties of a circular air jet impinging on a hot hemispherical surface. For various combinations of h/d, d/D, and Reynolds number, fluid flow, and heat transfer parameters were numerically determined.

2. Problem Description

The setup used in the present study is steady-state simulations in a two-dimensional heat transfer system of an air jet impinging on a hemispherical food product, as shown in Fig. 1. The analysis was done by using ANSYS Workbench 2020 R2. The fluid domain can be

considered axisymmetric about the jet centerline.

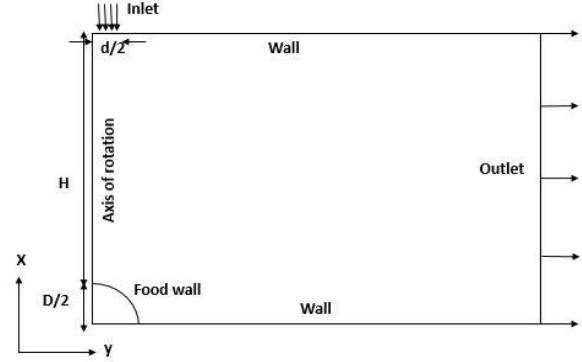


Fig. 1: The flow domain

The inlet section of the system has a diameter (d) of 30 mm and the hemispherical food a diameter (D) of 35 mm. The object's diameter does not vary, but the jet width does. The airflow through the impinging jet is considered to be a fully developed turbulent flow. For different Reynolds numbers (23,000 to 100,000), the ratio of jet to object distance, H/d (2 to 8) and the object surface curvature, d/D (0.57 to 1.286), the distribution of the local Nusselt number around the object is determined.

2.1 Governing Equation

The Navier-Stokes equations are a set of three fundamental equations that can be used to describe fluid flow and heat transport. The Navier-Stokes equations describe the conservation of mass, momentum, and energy in a fluid flow. In a turbulent flow, the magnitude of the velocity is important. It changes with time. Turbulence is the term for this change. Velocity in turbulent flow is subdivided into mean velocity (U) and turbulent component (u').

$$u_i = U_i + u_i' \quad (1)$$

The Navier-Stoke equations can be expressed as follows when turbulence is included in the velocity term. Continuity:

$$\frac{\partial \bar{u}_i}{\partial x_j} = 0 \quad (2)$$

Momentum:

$$\frac{\partial \bar{u}_i \bar{u}_j}{\partial x_j} = -\frac{1}{\rho} \frac{\partial \bar{p}}{\partial x_i} + \frac{\partial}{\partial x_j} \left[\nu_f \left(\frac{\partial \bar{u}_i}{\partial x_j} + \frac{\partial \bar{u}_j}{\partial x_i} \right) - \overline{u_i' u_j'} \right] \quad (3)$$

Energy:

$$\rho_f \bar{u}_j c_p \frac{\partial \bar{T}}{\partial x_j} = -\frac{\partial}{\partial x_j} \left[k_f \frac{\partial \bar{T}}{\partial x_i} + \rho_f C_p \overline{u_i' T'} \right] \quad (4)$$

Where, ν_f and ρ_f are the kinematics viscosity of the fluid (air in the present case) and density of the fluid respectively. The mean temperature and the fluctuating temperature of the fluid are defined by T and T' respectively. C_v is the specific heat capacity of the fluid at constant volume, and C_p is the specific heat capacity of fluid at constant pressure. K_f is the thermal conductivity of the fluid. The number of the unknown parameter in these turbulent flow equations is more than the number of equations due to the additional terms $\overline{u_i' u_j'}$.

This is referred to as the closure problem, which has been investigated for many years and many methods have been suggested to find solutions to these equations.

2.2 Meshing and Numerical setup:

ANSYS MESHING was used to mesh the data. The whole flow domain was divided into four section. Face

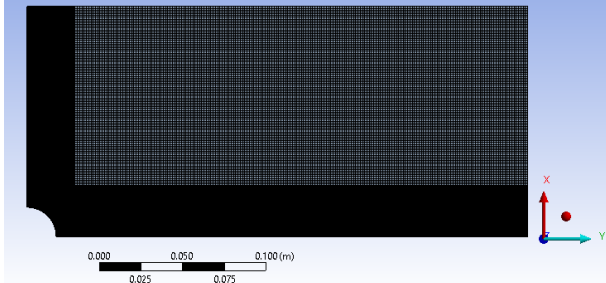


Fig. 2: Mesh of full flow domain

meshing was applied on each section of the flow domain. Also edge sizing was introduced for the particular parts of the flow domain.

2.3 Boundary condition and Material selection

A computational fluid dynamics (CFD) solution requires well-defined grid boundary conditions to model flow and heat transfer. At the inlet, the initial temperature of the air was set at 20°C. Jet velocity was calculated using the Reynolds number and hydraulic diameter of the jet. At the food wall boundary, a no-slip condition was used. The food surface was considered to be isothermal at 50°C for steady-state heat transfer solutions. Jet centerline was defined as the axis of rotation. It was determined that the outlet was a pressure outlet. The heat transfer from the food surface due to radiation was ignored. Also, viscous heat dissipation is neglected. Zero heat flux boundaries were assigned to all wall boundaries except the food surface. The exterior flow was connected with the food surface's wall boundary.

The material for the fluid was selected to be air at standard atmosphere having a density of 1.225 kg/m³ and viscosity of 1.7894*10⁻⁵kg/m-s. Thermophysical parameters of food material according to USDA (2000) composition data and the procedure suggested by Singh and Heldman (2001): $\rho = 1100 \text{ kg/m}^3$, $C_p = 3390 \text{ J/kg K}$ and $K = 0.55 \text{ W/m}$ [19].

3.0 Result and Discussion

3.1 Model Validation:

The impinging jet flow model was subjected to a detailed Mesh dependence test employing a variety of mesh elements. The outlet velocity obtained in the impinging jet flow is listed below in the following table.

Table 1 Outlet velocity for different no. of mesh elements

Mesh Elements	Outlet Velocity
432500	1.304
542500	1.302
673600	1.348
783680	1.306
880000	1.306

As it is observed from table 1 that for mesh elements 783680 the outlet velocity takes the value of 1.306. This value does not change much with the increasing no of mesh elements. So, the number of mesh elements 783680 can produce an accurate result with a very small deviation.

The simulated data is also validated with the data from Olsson, Ahrne, and Tragardh [12]. They used a slot air jet that was impinged on a circular cylinder. The slot jet had a width of 30mm and the diameter of the cylindrical food object was 35mm.

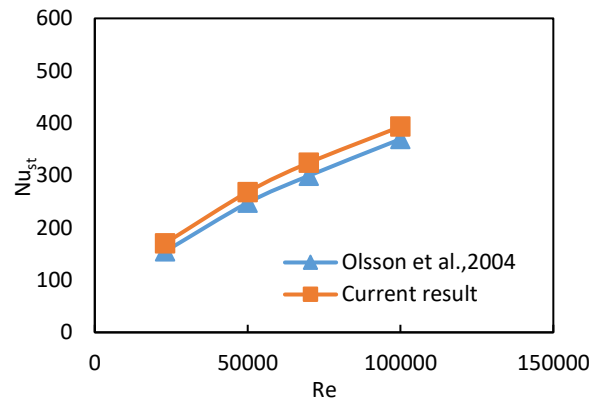


Fig. 3: Nusselt number variation with Reynolds number at the stagnation point

The change in the Nusselt number with the Reynolds number was validated with Ref. [12]. Fig. 2 shows a slight (6.46% to 10.16%) deviation from the reference result which is acceptable.

3.2 Effect of turbulence intensity (I):

The amount of turbulence near the jet exit has a substantial impact on jet dynamics, which impacts flow properties and thus heat transport phenomena along the target item to be cooled. It is clear from the graph that with increasing turbulence, the Nusselt number of the stagnation point rose for H/d=4, d=30 mm, and Re=23000, and also average Nusselt number value decreases, see figure 3, with increasing turbulence.

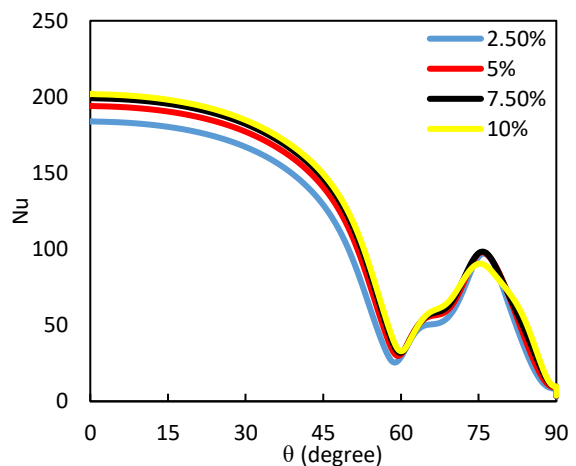


Fig. 4: Effect of turbulence in flow at the jet exit for d=30 mm, H/D=12 and Re=23000

3.3 Effect of Reynolds number:

The numerical simulation results are beneficial in getting the perception of the flow characteristics around the object. Figure 6 demonstrates the Nusselt number distribution over a hemispherical target for Reynolds numbers ranging from 23000 to 100000 where $H/d=4$, and $d/D=0.86$.

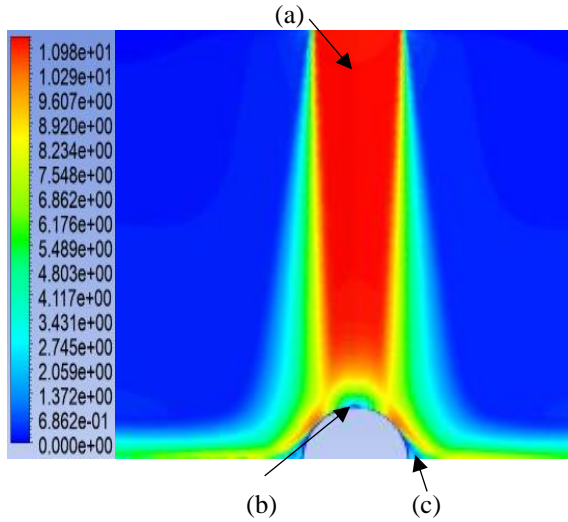


Fig. 5: Velocity contour in the flow domain

Figure 5 demonstrates the airflow in the computational domain. The flow in an air jet impinging on a surface might be ordered into three zones: free jet region, wall jet region, and stagnation flow region. Free jet (Figure 5, a) is the region where the jet centerline velocity is the same as the exit velocity of the jet from the nozzle. An increase in the static pressure is found, not shown in this study, when the jet approaches the stagnation point (Figure 5, b), where the local velocity of the jet is minimum. After the stagnation region, the flow follows the curvature of the cylinder until the separation zone (Figure 5, c).

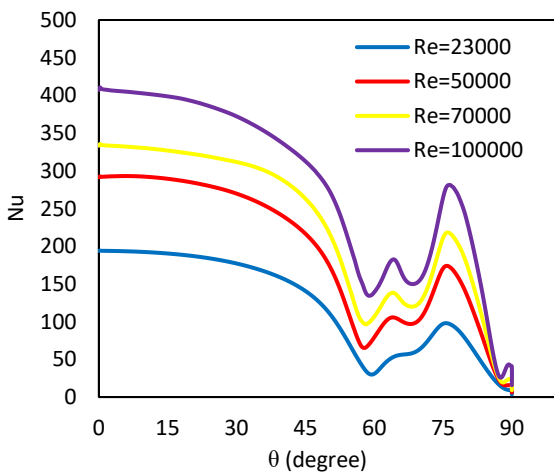


Fig. 6: Distribution of Nusselt number over the object for various Reynolds numbers at $H/d=4$ and $d/D=0.86$

A non-dimensional heat transfer coefficient is the Nusselt number. It heavily depends on the fluid channel's

geometry and heat transmission at the wall's boundary condition. There is a lot of turbulence in the stagnation point's flow, which results in a lot of heat transfer in the stagnation area. Heat transfer is minimized along the curved surface due to the proximity of the wall, and turbulence is likely reduced. The Nusselt number profile throughout the object's circumference revealed three maxima. This initial peak occurs around the stagnation point as the flow transitions from laminar to turbulent. The surface Nusselt number rapidly decreased after the first peak, until it reached the second peak position. The location of second peak was located near the flow separation zone. It was identified at a 55° to 70° angular distance from the stagnation point.

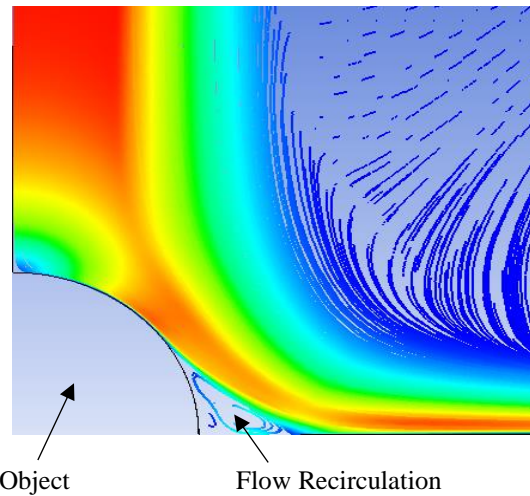


Fig. 7: Velocity contours with streamlines in the flow domain

The simulation results (Figure 7) indicate a flow recirculation zone below the separation point. This recirculation zone increases the heat transfer rate. Due to this phenomenon third peak (Figure 6) is greater than the second peak.

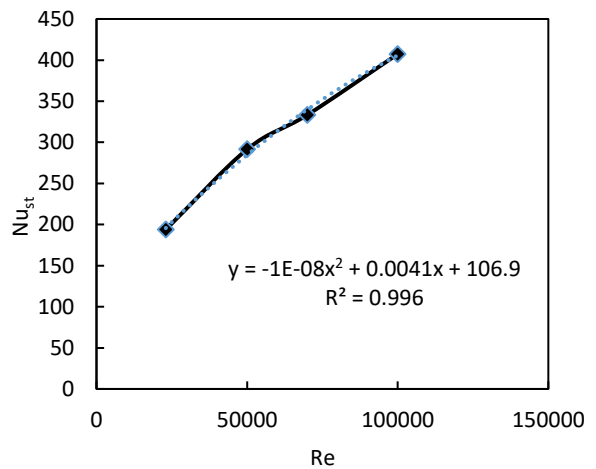


Fig. 8: Nusselt number variation with Reynolds number in the stagnation point at $H/d=4$ and $d/D=0.86$.

In turbulent flow, the boundary layer is correlated to the Reynolds number. Thus, the Nusselt number has a

relation with the Reynolds number. It is obvious from figure 6 and figure 8 that the Nusselt number increases with an increase in the Reynolds number.

3.4 Effect of H/d:

The effect of H/d (jet to object distance) on Nusselt number variation over the object was studied.

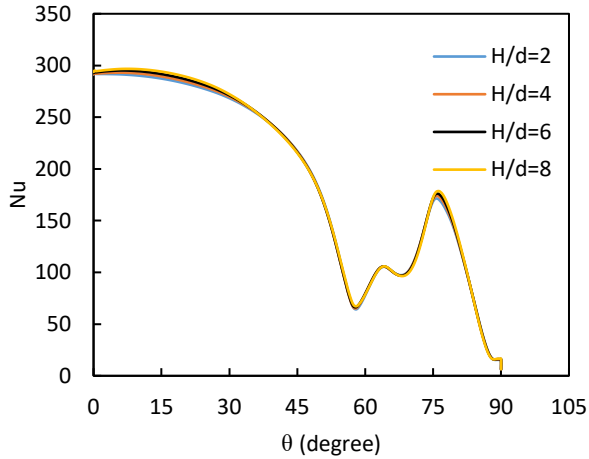


Fig. 9: Nusselt number variation over the object for different H/d, at Re=50000 and d/D =0.86

Figure 9 shows that heat transfer at the constant Reynolds number and surface curvature does not seem to depend remarkably on jet-to-object distance (H/d).

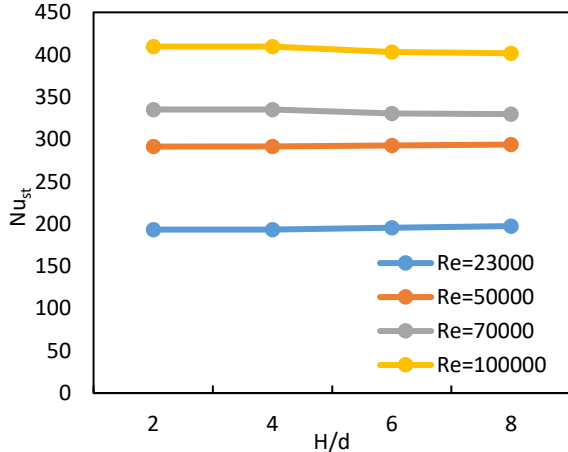


Fig. 10: Stagnation point Nusselt number variation with H/d for different jet Reynolds numbers.

Figure 10 also shows that the distance between the jet and the object (H/d) has relatively little effect on the Nusselt number distribution over the food object. With H/d, the Nusselt value at the stagnation point does not fluctuate much. Therefore, the Nusselt number appears to be unaffected by H/d.

3.5 Effect of d/D:

The effect of surface curvature (the ratio of jet width to cylinder diameter) has also been investigated. The Nusselt number variation over the object and in the stagnation point is affected by the surface curvature.

Figure 11 shows that the Nusselt number decreases as the surface curvature increases, in contrast to what is reported by Olsson et al. [12]. Their study involves a complete circular cylinder in which angular distance varies from 0° to 180° whereas this current study involves only a hemispherical cylinder as a food object.

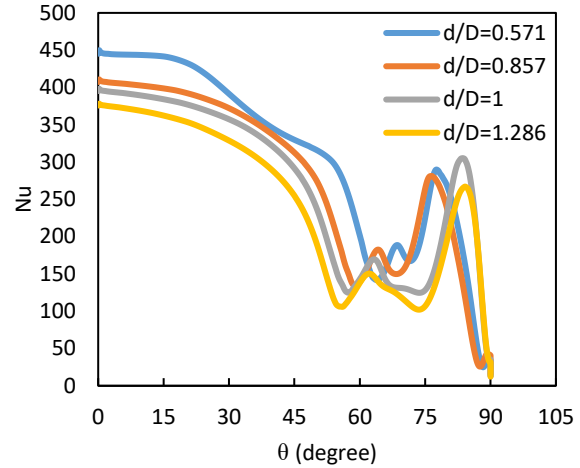


Fig. 11: Nusselt number variation over the object for different d/D, Re=100000 and H/d =4

The variation of stagnation point Nusselt number with respect to Reynolds number at different surface curvature (d/D) for a constant jet to object distance (H/d=4) was also investigated. Figure 12 shows that the stagnation point Nusselt number decreases as the surface curvature increases.

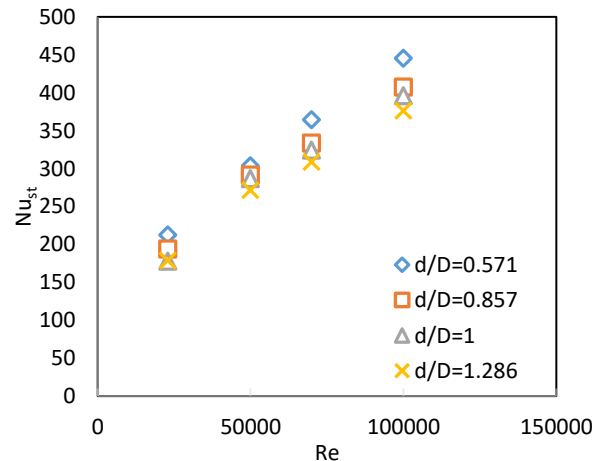


Fig. 12: Reynolds number vs stagnation point Nusselt number at different d/D for H/d=4

In the case of fixed H/d and Re, the jet velocity is higher and the mass flow rate is lower with a smaller nozzle diameter than with a larger d. The Nusselt number at the stagnation point is greater because of the quicker velocity at lower d (and consequently d/D). However, when compared to a larger nozzle diameter, for example, the local Nusselt number decreases dramatically in circumferential directions due to the reduced mass flow rate of the jet.

4.0 Conclusion

The heat transfer and fluid flow caused by a circular jet striking hemispherically shaped food that is resting on a surface were examined using numerical analysis. Reynolds number, the curvature of the object's surface, the amount of turbulence at the jet exit, and the separation between the jet exit and the object have all been investigated as potential influences. According to the distribution of surface heat transfer coefficient, heat transfer is maximum in the deposition area and lowest in the bottom part of the element. The stagnation and local Nusselt numbers increase with increasing Reynolds number and decrease with increasing surface curvature, but these parameters are not affected notably by the distance between the jet and the object. Additionally, nozzle design plays an important role in determining the flow variables, especially the magnitude of the turbulence at the jet outlet. A detailed study of the nozzle shape and its effect on the dynamics of the flow will provide further insight into the cooling process.

5.0 Reference

- [1] J. Lujan, R.G. Moreira and Y.J. Seyed, "Air impingement drying of tortilla chips", *Drying Technology* 15(3&4): 881-897, 1997.
- [2] R.Borquez, W. Wolf, W.D. Koller and W.E.L. Spieb, "Impinging jet drying of pressed fish cake", *Journal of Food Engineering* 40(1-2): 113-120, 1999.
- [3] G. Scott & P. Richardson, "The application of computational fluid dynamics in the food industry", *Trends in Food Science and Technology* 8(1997) 119-124.
- [4] B. Xia & D.W. Sun "Applications of computational fluid dynamics (CFD) in the food industry: A review", *Computers and Electronics in Agriculture* 34(2002) 5-24.
- [5] Twanda Marazani, Daniel M. Madyira and Esther T. Akinlabi, "Investigation of parameters governing the performance of jet impingement quick food freezing and cooling systems: a review", *Procedia Manufacturing* 8 (2017) 754-760.
- [6] J.P. Bouchez and R.J. Goldstein, "Impingement cooling from a circular jet in a cross flow." *International Journal of Heat and Mass Transfer* 18(1975) 719-730.
- [7] C. Cornaro, A.S. Fleischer and R.J. Goldstein, "Flow visualization of a round jet impinging on cylindrical surfaces." *Experimental Thermal and Fluid Science* 20(1999) 66-78.
- [8] C. Gau and C.M. Chung, "Surface curvature effect on slot air jet impinging cooling flow and heat transfer processes." *ASME J. of heat transfer* 113(1991)858-864.
- [9] Jung-Yang San, Chih-Hao Huang and Ming-Hong Shu, "Impingement cooling of a confined circular air jet", *Int. J. Heat Mass Transfer*. Vol. 40, No. 6, pp. 1355~1364, 1997
- [10] Carmela Dirita, Maria Valeria De Bonis and Gianpaolo Ruocco (2006), "Analysis of food cooling by jet impingement, including inherent conduction", *Journal of Food Engineering* 81 (2007) 12-20.
- [11] F.Gori and L.Bossi, "On the cooling effect of an air jet along the surface of a cylinder", *Int. Comm. Heat Mass Transfer*, Vol. 27, No. 5, pp. 667~76, 2000
- [12] E.E.M. Olsson, L.M. Ahrne and A.C. Tragardh, "Heat transfer from a slot air jet Impinging on circular cylinder", *Journal of Food Engineering* 63 (2004) 393-401.
- [13] S.K. Singh and R. Paul Singh (2008), "Air Impingement Cooling of Cylindrical Objects Using Slot Jets"
- [14] N. Nitin, R.P. Gadiraju and M.V. Karwei, "Conjugate heat transfer associated with a turbulent hot air jet impinging on a cylindrical object", *Journal of Food Process Engineering* 29 (2006) 386-399.
- [15] S.H. Kang and R. Greif, "Flow and heat transfer to a circular cylinder with a hot impinging air jet", *Int. J. Heat Mass Transfer*. Vol 35. No. 9. pp 2173-2183, 1992
- [16] Qiang Guo, Zhiwen and Ruifeng Dou (2016), "Experimental and numerical study on the transient heat transfer characteristics of circular air jet impingement on a flat plate", *International Journal of Heat and Mass Transfer* 104 (2017) 1177-1188.
- [17] T.L. Chan, C.W. Leung, K. Jambunathan, S. Ashforth-Frost, Y. Zhou and M.H. Liu, "Heat transfer characteristics of a slot jet impinging on a semi-circular convex surface, *International Journal of Heat and Mass* 45(2002) 993-1006
- [18] Dae Hee Lee, Young Suk Chung and Moo Geun Kim, "Turbulent heat transfer from a convex hemispherical surface to a round impinging jet", *International Journal of Heat and Mass Transfer* 42(1999) 1147-1156
- [19] Dushyant Singh, B. Premachandran and Sangeeta Kohli (2013), "Experimental and numerical investigation of jet impingement cooling of circular cylinder", *International Journal of Heat and Mass Transfer* 60(2013) 672-688.

NOMENCLATURE

Cp	Specific heat (J/(kg°C))
d	Width of jet (m)
D	Diameter of object (m)
d/D	Surface curvature
h	Heat transfer coefficient (W/(m ² °C))
H	Jet distance (m)
H/d	Jet-to-cylinder distance
K	Thermal heat conductivity (W/(m °C))
Nu	Nusselt number (Nu=hd/k)
P	Pressure (Pa)
Re	Reynolds number
T	Temperature (°C)
U	Averaged velocity (m/s)